CHAPTER V

IN VIVO ASSESSMENT OF TIOPRONIN MONOLAYER PROTECTED GOLD CLUSTERS FOR IMMUNOGENICITY, DISTRIBUTION, AND TOXICITY

Introduction

Nanotechnology is a rapidly growing field with uses in imaging and vaccinating against human diseases. Before monolayer protected clusters can be used more extensively for *in vivo* applications, their pharmokinetic behavior must be fundamentally understood. This would include factors like clearance routes and time, retention within organs, dosage based toxicity, and immunogenicity. Herein, tiopronin monolayer protected clusters (TMPCs) are subcutaneously injected in a mouse to evaluate these factors in a model system. The concentration of nanoparticles is monitored in blood and urine along with affects on red and white cell counts for immunogenic properties. Furthermore, it is determined in what organs TMPCs tend to localize and what concentrations are appropriate to avoid deleterious side-effects. Urinalysis provided detailed information on kidney function, while organ histology elucidated cellular effects on the liver and kidney.

Monolayer protected nanoparticles (MPCs) lend themselves to a variety of applications based on their ability to be functionalized using facile synthetic methods.[1-4] While most research focuses on their electrochemical, optical, and catalytic properties, a growing body of work is shifting toward their biological applications.[5] Particularly, some of the potential uses are *in vivo* based imaging[6-9], targeting,[10-12], radiotherapy,[13,14] and

synthetic vaccines.[5,15] However, before MPCs can be used for developed applications, their effect in a living system must be well characterized.

A major component to the hindrance of nanotechnology applications is the question: How do the new materials differ from their constituents? Since MPCs are a composite of two non-toxic materials (Au^0 core with a tiopronin ligand coating), it must be understood how the new product responds. The ligand, tiopronin, is a commonly used therapeutic for treating a variety of conditions like rheumatoid arthritis, hepatic diseases, and cystinuria under the trade name Thiola.[16-18] Similarly, low toxicity gold complexes, like auranofin, were commonly employed with small ligands for relief from rheumatoid arthritis.[19] However, much like recent reviews of carbon nanotubes, the nanomaterial could have distinct toxicological properties compared with the starting chemical components.

Before gold MPCs can really be used for applications, an in depth study must be performed to evaluate toxicity, retention times, and immunogenicity.[20-23] Recently, groups have looked at how variations in ligands and core size change clearance. Since clearance time and path are of the utmost interest, variability in these parameters is critical.[9,21,24-27] Ligands can be selected based on charge and length,[10,21,28] while cores can be varied in size and metal composition, either different metals or a mixture.[25,27,29] Short retention times prevent any useful information because the particle does not reside long enough for imaging or for immunogenic response. However, extended retention times can lead to increased toxicity due to excessive accumulation.[30] Therefore, a tailored particle needs to circulate long enough for useful imaging or to elicit an immune response, but not so long to cause toxicity.[21,27]

Extensive work has been done by Choi *et al.* in tailoring quantum dots for optimized *in vivo* usage.[21] Through his work he postulated a series of criteria for nanoparticles to maximized efficacy and reduce their toxicity. One of the constraints is to construct the nanomaterial (nanoparticle) with only non-toxic components. In continuation of this, a biodegradable composite would also work well too because it would break down and be cleared from the body with little to no effect. Besides material concerns, the particles should be tailored to achieve a certain hydrodynamic size, which Choi theorizes should be below 5.5 nm. This smaller size allows for a higher percentage clearance, and conversely, lower retention.

There are a variety of methods for examining *in vivo* circulation, clearance, and retention of gold nanoparticles.[31] Inductively coupled plasma with a mass spectrometry detector (ICP-MS) is a very sensitive technique for evaluating heavy metal concentrations[32-34] and has seen recent growth in nanotechnology.[35] The instrument utilizes an argon plasma flame to ionize the metals before they are sent to the mass analyzer. For many metals, there are interferences present from overlapping masses, however, gold is free from interference making sample preparation more straightforward. Gold has been analyzed using a variety of conditions, from 2% nitric to a mixture of nitric and hydrochloric acid.

To evaluate these aforementioned aspects, gold MPCs with tiopronin capping ligands were synthesized with average diameters around 2.4 +/- 0.6 nm. This size regime should fit the criteria suggested by Choi *et al.* for clinically relevant nanoparticles, in that they fit the 5 to 15 nm hydrodynamic range and are composed of non-toxic, easily cleared

components.[21] Additionally, a size separated group of these MPCs was used to further test the hypothesis of clearance versus particle diameter.

Experimental

Materials

N-(2-Mercaptopropionyl)glycine (tiopronin) was purchased from Sigma. Sodium borohydride (98%) was purchased from Acros Organics and used without further purification. Sodium phosphate, methanol (ACS), acetic acid (ACS), and 15 mL sterile conical vials were purchased from Fisher Scientific. Sterile phosphate buffer was from Mediatech. Gold tetrachloroauric acid was synthesized in house from 99.99% gold shot. Water was purified by an 18 MΩ Solution 2000 water purification system.

Synthesis of Tiopronin Monolayer Protected Clusters (TMPCs)

TMPCs were synthesized using the modified Brust reaction described by Templeton.[3,36,37] Briefly, 1.0 g of $HAuCl_4 \cdot 3H_2O$ was added to a 100 mL mixture of 6:1 methanol:acetic acid (v/v). The mixture was placed in ice and stirred for 20 minutes. Tiopronin was added in 3:1 mole excess (1.2 g), and stirred for another 20 minutes, yielding a ruby red solution that begins to fade toward yellow. At this point, sodium borohydride (1.1 g), dissolved in a minimum of water, was added to the solution in 10x mole excess to gold. The reaction stirred overnight at room temperature, and then the volume was then reduced to 20 mL by rotovaporation. The solution is then adjusted to pH ~1 by the addition of concentrated HCl. Next, the solution was dialyzed against 4 L

of DI water, changed twice daily, for 5 days using 10,000 MWCO dialysis tubing. After 5 days, samples were checked for impurities using NMR and, when pure, were rotary evaporated to dryness and stored.

Core sizing of TMPCs

Nanoparticles were measured using a Phillips CM20T transmission electron microscope (TEM), operating at 200 keV at a magnification of 414 kx. Samples were prepared by dissolving 1 mg of dried particles in 5 mL of dionized water, sonicating for 10 minutes, and then dropped onto ultrathin carbon grids (400 mesh, Ted Pella, Inc.). Results are reported using the mean +/- the standard deviation obtained from negatives measured by ImageJ (NIH, http://rsb.info.nih.gov.ij/) using sample sizes of no less than 50 nanoparticles.

Thermogravimetric Analysis (TGA) of TMPCs

Thermogravimetric analysis of TMPCs was performed on an Instrument Specialist's TGA-1000 using platinum sample pans. Weight loss as a function of temperature was carried out from 25 to 900 ºC using ~8 mg of dried sample, with a temperature step of 20 ºC per minute (an additional 15 minute hold at 100 ºC was to assure all the water is evaporated). Compressed air was used as the purge gas, with a flow rate of 60 mL/min.

Animal Models

Animals were housed in a Division of Animal Care (DAC) facility, fully certified by the Association for Assessment and Accreditation of Laboratory Animal Care (AALAC). Animals were kept under supervision of full time veterinarians and support staff, with an approved IACUC protocol. BALB/cAnNHsd mice, 5-6 wk, weighing 15-16 g were purchased from Harlan Laboratory. All animals were allowed to acclimate to the DAC facility for one week before experimenting. Following the acclimation, the mice experiments followed the timeline in Figure 40. Nanoparticles were prepared in sterile saline buffer (n = 10 mice per concentration group) and injected subcutaneously. Dosage concentrations were 10, 20, 30, 40, 60, and 120 μM, using a 200 μL injection volume. Blood was drawn using submandibular bleeding techniques, in compliance with our protocol and NIH bleeding guidelines of mL/kg body weight per 2 weeks.[38,39] Urine

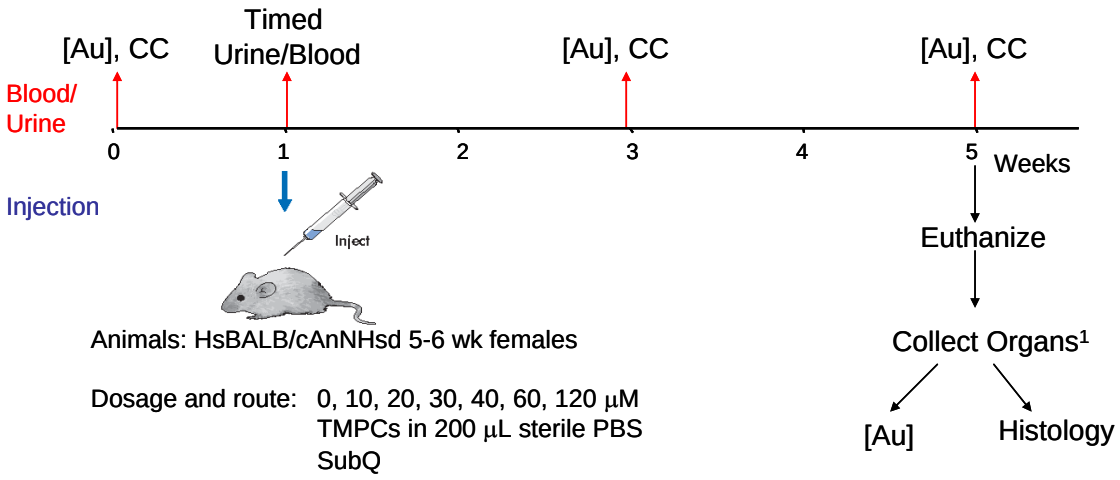

[Au] = ICP-MS, 2% HNO_3
CC = Coulter Counter of RBC/WBCs
1. Kidney, Liver, Spleen, Heart, Lungs

Figure 40. Experimental timeline showing the days of mouse injections, bleeds, , and urine collection.

was collected on cellophane at the same time point as the blood, being careful to avoid fecal contamination.[40] At the end of the experiment, mice were euthanized using CO_2 followed by cervical dislocation. Blood samples were divided between ICP-MS and coulter counter, and organs were harvested immediately after euthanasia for histology and trace metal analysis. Urine was tested for both gold content and select biological indicators (*see urinalysis)*.

ICP-MS of blood, urine, and organs for gold content

Blood and urine samples were prepared in a similar manner. Briefly, 5 μL of blood or urine fluid were diluted in 10 mL of 2% nitric acid (Optima grade, Fisher Scientific). Organs were excised, weighed (for normalization), and dissolved in concentrated nitric acid (70% HNO_3), and heated until all the acid boiled off and the samples were dry. The dry sample was then reconstituted in 10 mL of 2% nitric acid as with the blood and urine. Samples were then run on an ELAN DRC II ICP-MS. Calibration curves were created using TMPCs from the same synthesis to correct for different ionization characteristics.

Coulter Counter for red and white blood cells

Cell counts were obtained for both red (RBCs) and white blood cells (WBCs) using a Beckman Z1 Coulter Particle Counter. From the whole blood sample, 20 μL of blood was diluted into 20 mL of Isoton® II diluent (Beckman Coulter) to create the WBC solution. Next, 200 μL of WBC solution was transferred to 19.8 mL of diluent, this solution was used as prepared for the RBC count. In the WBC solution, 15-drops of Zap-

Oglobin II lysing agent (Beckman Coulter) were added and then the solution was allowed to sit two minutes until the color changed from red to yellow, at this point it was ready for analysis.

Urinalysis

Urine was tested for ten components within 1 hour of collection by using Multistix 10 SG reagent strips (Siemens, Tarrytown, NY). Single droplets of urine were placed on individual reagent blocks to test for glucose, bilirubin, ketone, specific gravity, blood, pH, protein, urobilinogen, nitrite, and leukocytes.

Histology

Organs were excised shortly after euthanasia and sections of kidney and liver were set aside. These sections were fixed using formalin, 10% neutral buffered with 0.03% eosin (Sigma-Aldrich) and sent to Vanderbilt's histology core for H&E staining. The resulting slides were interpreted for trauma to the various tissues with the significant help of Dr. Ken Salleng, DVM.

Size-Dependent Clearance

Previously, it has been reported that size can be a critical factor in nanoparticle's biological effects.[21] The particles were separated using a 30k MWCO filter to remove the larger cores and any possible aggregates. The particles were imaged with TEM and found to be statistically different in size using a Student's t-test. Then different groups of

mice were dosed at 20, 30, 40, and 60 μM concentrations to mirror the first half of the study.

Results and Discussion

Tiopronin protected nanoparticles were characterized using four standard methods. First, we evaluate purity based on NMR by looking for broadening of all tiopronin peaks, indicating excess free ligands have been removed along with any solvents that could have potential biological effects. The particles are next sized using both UV-Vis and transmission electron microscopy. TEM is used to evaluate discrete sizes, aggregation, and create our population histogram. UV-Vis is an estimation of size based on the surface plasmon band (SPR), which will give an idea of average diameter above or below 5 nm and serves to compliment TEM. To determine organic ligand composition, thermogravimetric analysis (TGA) shows a mass loss of 31% percent of organics. In running these techniques, the average composition of the MPC was determined as $Au_{260}Tiopronin_{213}$.

Figure 41 shows a calibration curve consisting of TMPCs in nitric acid. The x-axis represents the concentration of TMPC solution as prepared, while the y-axis is the concentration recorded from the instrument. A typical calibration showed approximately 30% less particle (dark color) than there should have been. This can be attributed to the tiopronin monolayer which contributes mass, but does not show up in the ICP-MS because of its organic composition. The lighter shade is the addition of the 30% organic, which reconciles the difference in concentrations.

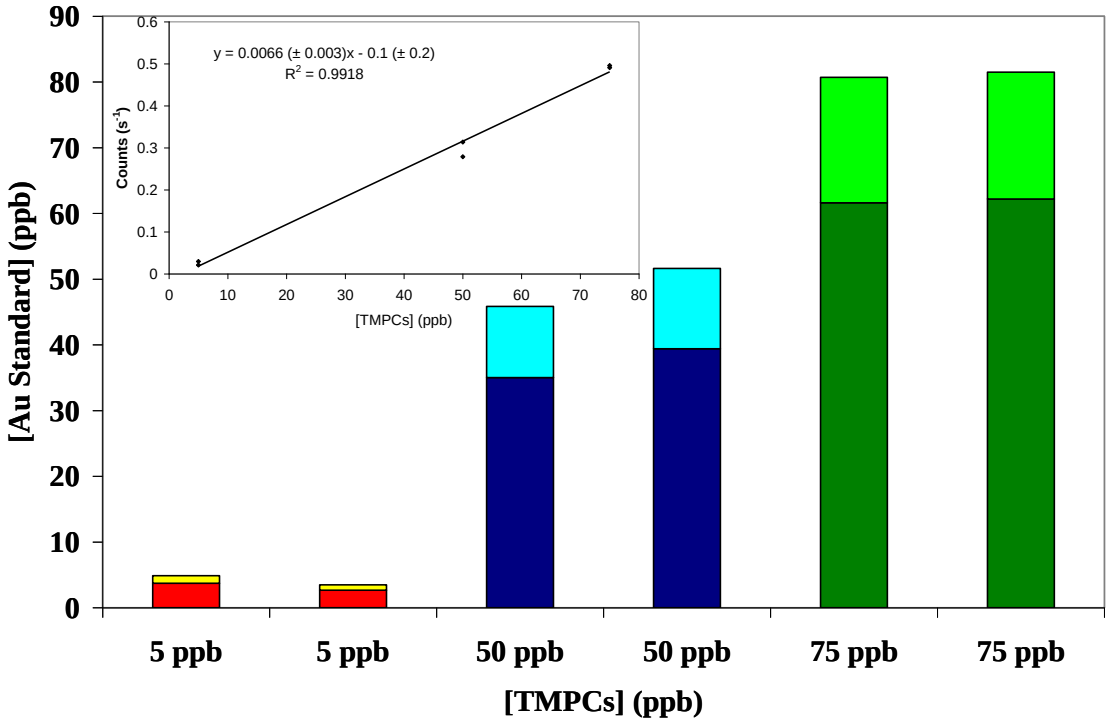

Figure 41. Calibration curve for TMPCs analyzed by ICP-MS. The x-axis is the concentration of the solution as made and the y-axis is the concentration determined by the ICP-MS. The lighter shades are the addition of the 30% organic layer.

All the studies are carried out with this single composition of particle. Injection solutions are made in sterile phosphate buffered saline (PBS), using only sterile syringes. Injected solutions are 200 μL in total volume and composed of a range of concentrations (0-120 μM) to determine the most effective response per dose. After particles were injected subcutaneously, blood and urine are collected at time points to monitor blood circulation and renal clearance, respectively. Using these collections, a concentration vs. time profile visually shows overall TMPC concentrations. At the same time, a plot of survival rates helps to monitor what doses are safe, shown in figure 42.

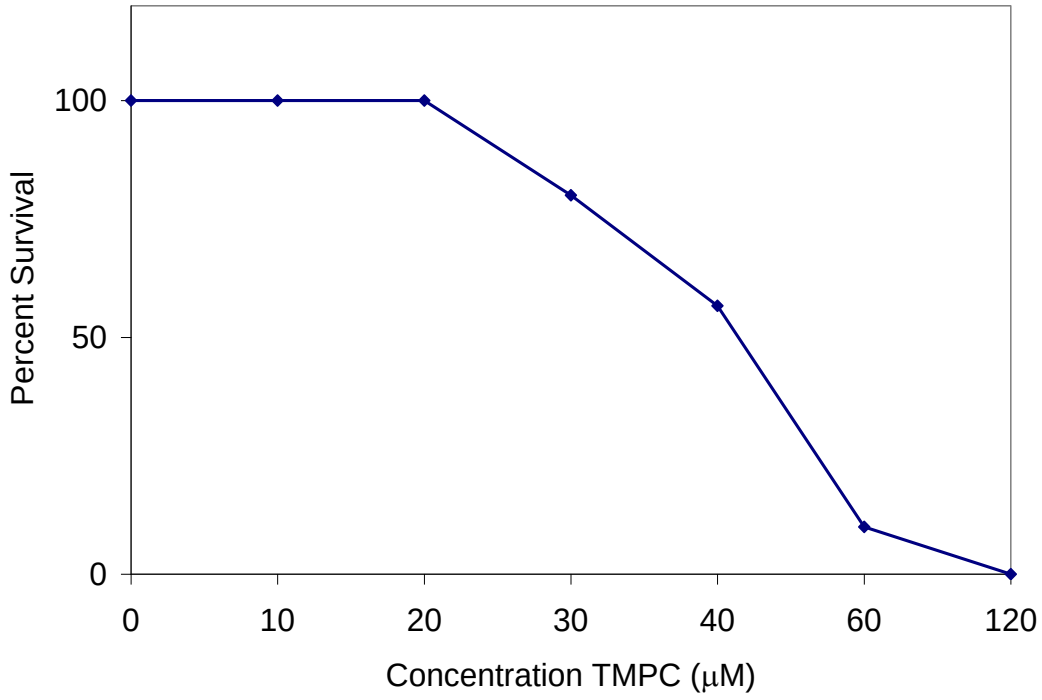

Figure 42. Concentration versus survival profile for the mice injected with TMPCs. 40 μM is the approximate LD50 concentration

The biological toxicity of nanomaterials can be linked to the retention and clearance from the body. One of the likely clearance routes for nanomaterials is through renal filtration into the urine. Urine is collected directly following injection for the next 96 hours. From these plots, the total renal clearance lands within 48 hours, with the vast majority cleared in the first 8 to 24 hours for the lowest concentrations, seen in figure 43. However, while the concentration drops rapidly from 10,000+ ppb to 100 ppb in the 60 and 120 μM groups, these mice exhibited the highest mortality rate, which could indicate that overly rapid clearance is detrimental to the renal tissue. Meanwhile, the mice with more consistent gold excretion have higher survival percentages. After 96 hours, the concentration in urine returns to pre-injection quantities of 1 to 20 ppb. This indicates that the particle's excretion does reach a minimum state, which is an important aspect for further use.

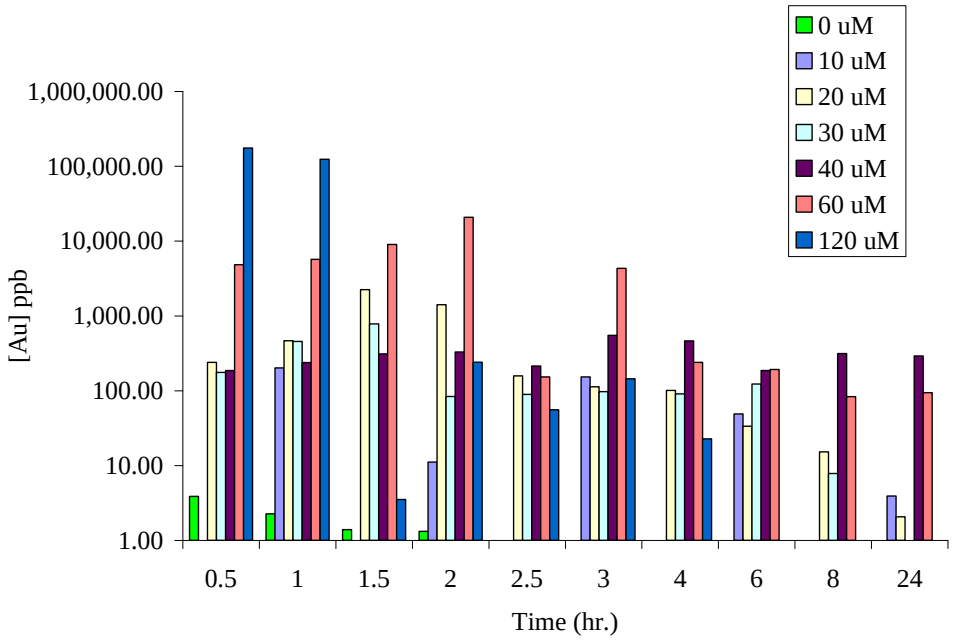

Figure 43. The decrease in urine plotted versus time. At 120 mM there is a rapid drop off in concentration. At lower dosages (0, 10, and 20 mM) the excreted concentration is stable until 24 hours.

In addition to urine, blood was analyzed for its gold content as a direct means of measuring circulation time, shown in Figure 44. Much like the urine profile, a decrease is noted during the 24 hours of collection, especially at the highest injected concentrations. This decrease correlates well with the urine data, as the mouse's filtration system has already removed the bulk of the nanoparticles, therefore, leaving less for circulation. Again though, the mice with the fastest decrease in concentration exhibited the most dramatic effects. The mice at 0-40 mM had fairly uniform concentrations for the 24 hour period, but by 2 weeks showed no further nanoparticle circulation. Perhaps the most puzzling data was the 120 mM group, which shows virtually no gold content for the limited samples that could be obtained before euthanizing the group. Meanwhile, the urine showed a dramatic change in concentration,

starting from above 100,000 ppb, with the blood never exceeding 50 ppb. These mice show the highest levels of distress, starting eight hours after injection, unlike other groups

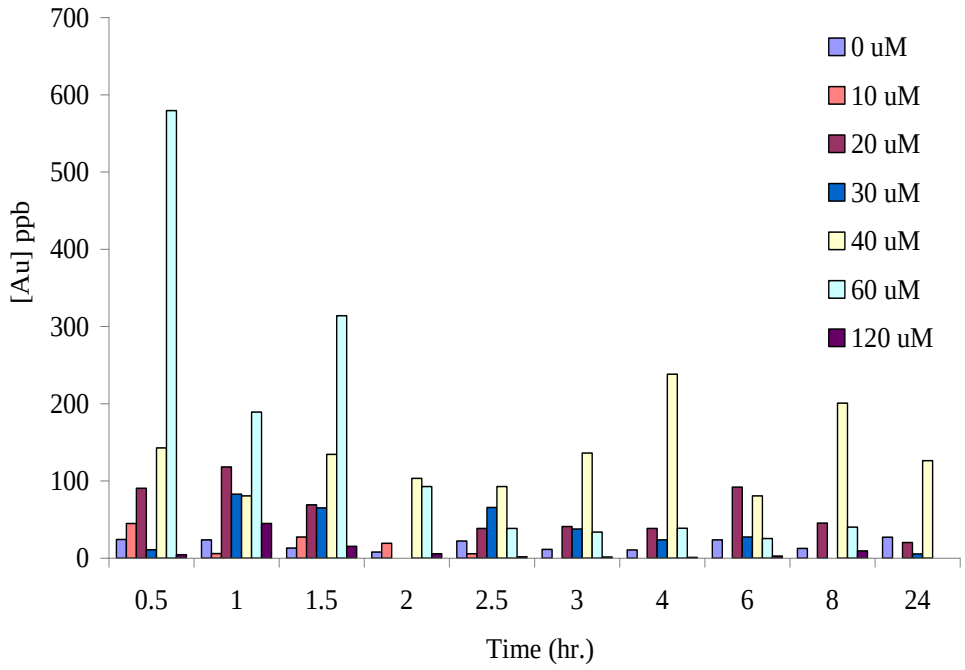

Figure 44. The clearance profile showing a decrease of TMPCs in blood over a 24 hour period, based on concentration. There is a good correlation between injected concentration and blood levels. The only exception is the 120 μM population, which shows an almost complete lack of nanoparticles in the blood.

which have a minimum time to symptoms of at least three up to seven days (60 and 40 μM, respectively).

The concentration dichotomy between blood and urine at high doses presents an interesting possibility that the particles may aggregate from opsonization with blood proteins, causing the filtration system to work harder and possibly block renal tubules from functioning properly. A follow-up study looked at mixing nanoparticles into whole

blood and monitoring for aggregation size changes by UV-Vis. Our results show that after 72 hours none of the particles begin to precipitate or form larger aggregates. This suggests the particles are either cleared or retained as individual clusters. Figure 45 shows the UV-Vis data collected over a 22 hour period, corrected with a baseline scan of

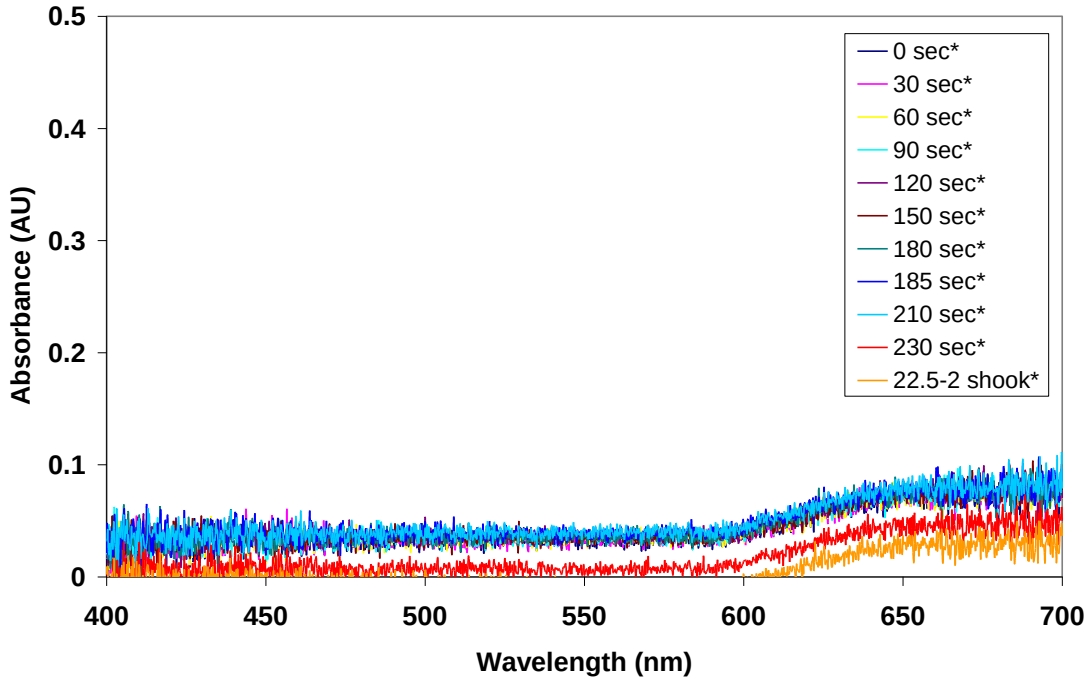

Figure 45. UV-Vis spectra over a 22 hour time period which shows no appearance of an SPR band.

blood without TMPCs. During this time no SPR band develops, which would indicate larger particles.

Outside of blood and urine clearance, the particles can also be retained in the organs. The main filtration organs are the kidneys and liver, while the spleen is blood rich and important for recycling red-blood cells. The heart is also examined because of

the heavy blood flow. The results, which are corrected for differences in weight, show that the liver retains the most TMPCs followed by the spleen and kidney. This matches with the organ functions since the liver processes blood for toxins. The spleen is responsible for recycling RBCs and the kidneys filter the blood for waste. These two organs show the next amount of gold, followed by the heart. The organs retentions are shown in Figure 46, based on their dosage concentration. Initially lungs were tested,

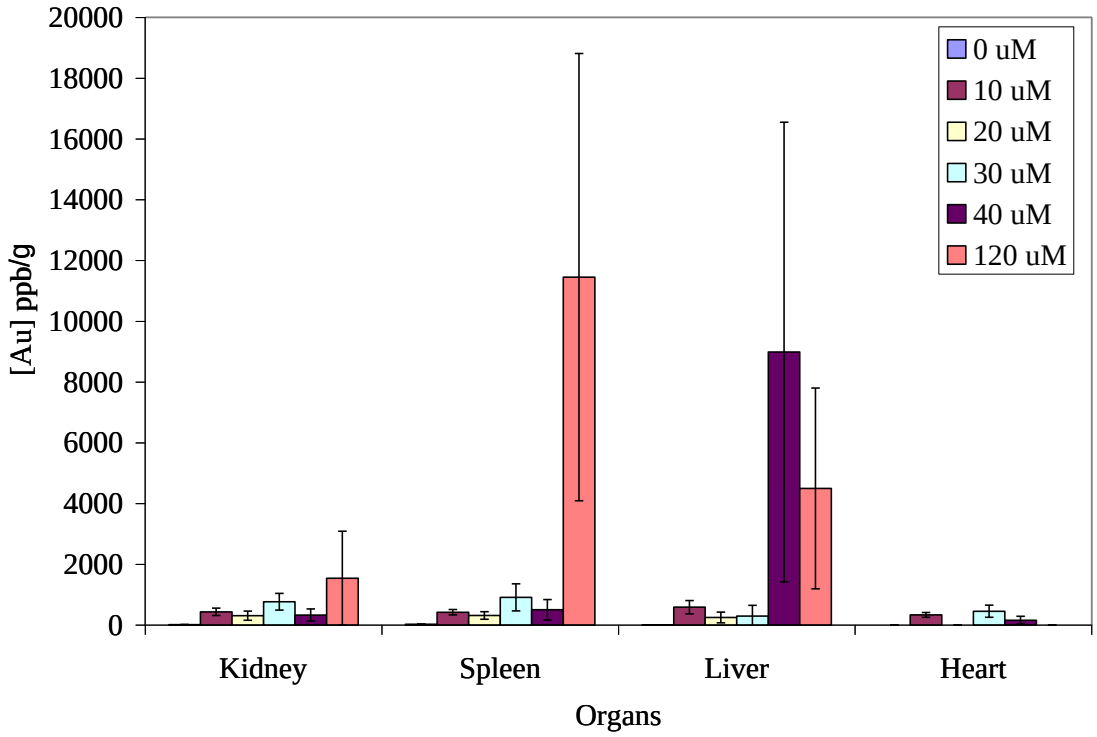

Figure 46. Summary graph of all the organs according to their gold exposure. The spleen and liver show the most gold on a gram-to-gram comparison.

however, they show no accumulation of the gold so further testing ceased. The spleen dosage at 120 μM is believed to be extremely high because the mice were euthanized so quickly after injection. There may not have been enough time for the TMPCs to be cleared from the blood and urine.

While gold concentrations are a key aspect to measure, there are also biological markers that can indicate the nanoparticle's effect on the body. One such parameter to evaluate is the red and white blood counts (RBCs and WBCs). Cells counts are measured using a coulter counter to look at the potential immunogenicity of the TMPCs. Changes in the counts, especially WBCs, indicate that the particles may or may not stimulate the immune system. The coulter counter results indicate that, in low doses, the particle itself does not cause a statistically relevant change in red or white cell counts, nor their ratio, during a four week period, seen in Figure 47. However, the trend shifts at the 40 μM level, with a spike at the two week sampling. The increased ratio suggests the particles are actually suppressing the WBCs based on the cell counts.

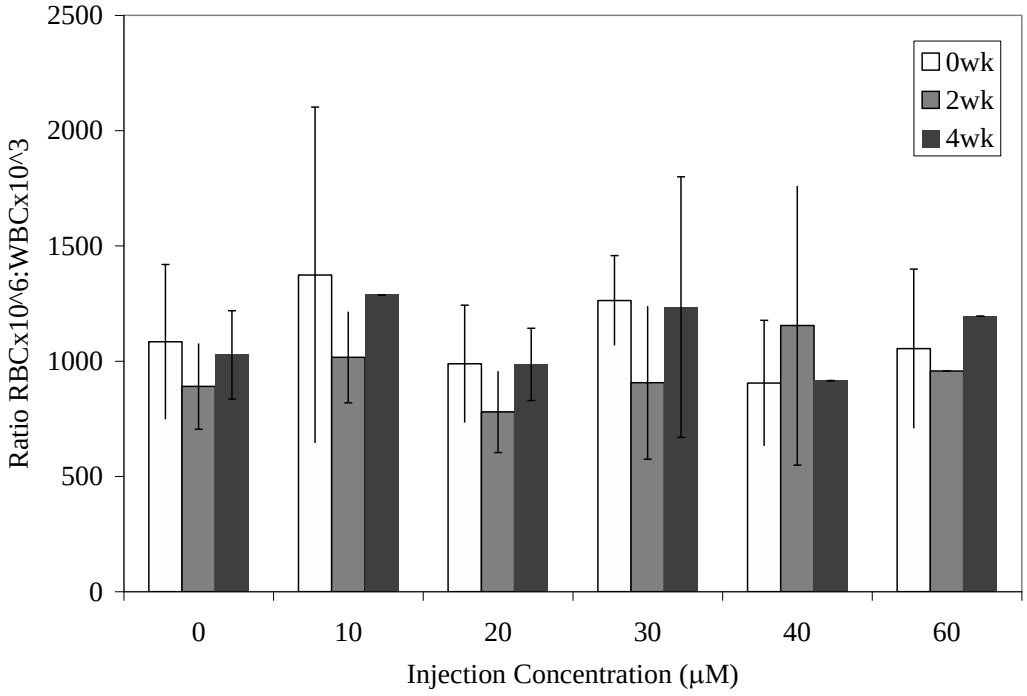

Figure 47. Coulter counter results from the ratio of RBC to WBC over a 4-week period. The 120 μM group is not shown because no mice survived the full experiment.

There are also sets of biological markers carried in the urine. These makers are excreted as the nanoparticles are filtered through the kidneys. Specifically, the interest is in total protein, leukocytes (WBCs), RBC, specific gravity, pH, and nitrite levels. Increased amounts of these markers can indicate kidney damage or even infection (from non-sterile injections) in the case of nitrites. Over the time course of 24 hours, there were increased levels of these markers trending with concentration. At 40, 60, and 120 μM there are increased levels of protein, RBCs, and WBCs. These three markers show that the particles are causing some extent of tissue damage to the kidneys as they passage. The lack of nitrites with WBCs means the sterile practices did not lead to infection during the course of the experiment.

These markers only serve as an example for what passes through the body and is in the urine stream. They do not, however, show the physical damage to the organs,

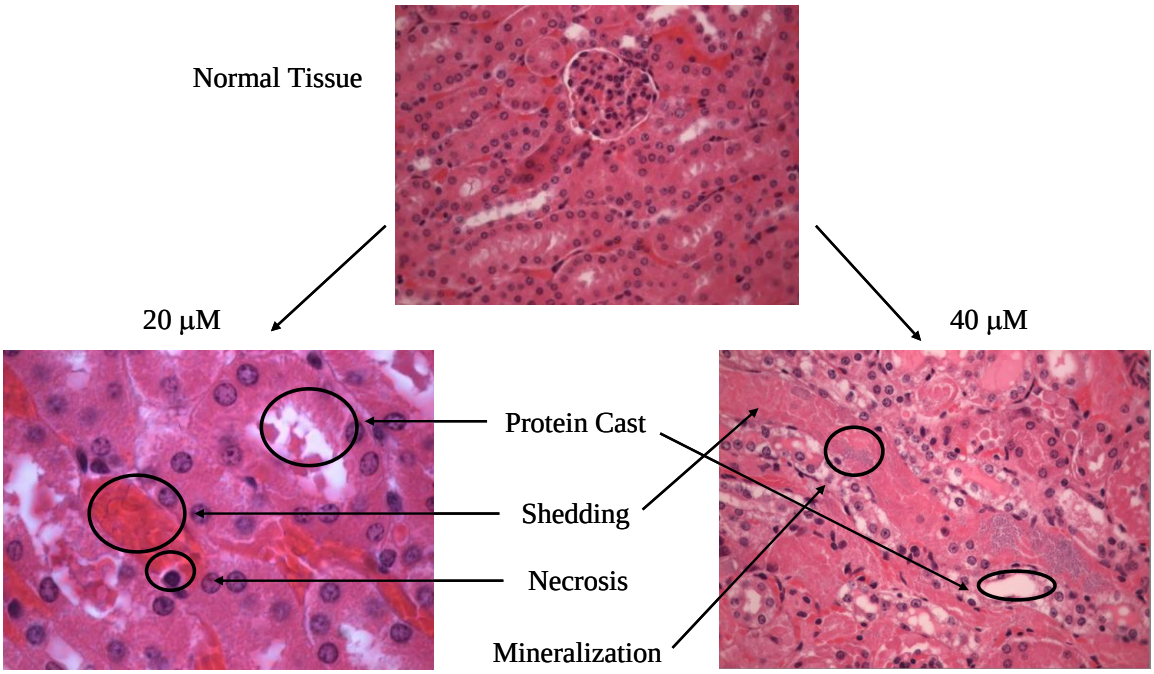

Figure 48. Representative histology slides from mice at that were dosed at 0, 20, and 40 μM. Kidney damage can be seen at the higher concentrations.

namely the kidney and liver. A more concrete picture is obtained by sectioning organs, staining them, and visually inspecting them under a microscope. Tissue samples were sent for histological analysis at Vanderbilt's Division of Animal Care. At lower concentrations of nanoparticles, there appeared lessened amounts of renal damage, which matches the survival curve. However, only the saline group showed no tissue damage to the kidneys. Upon higher dosages the kidneys begin to show mild to severe necrosis, shedding of tubules, and blood loss. The slides in Figure 48 show the tissue necrosis at 20 and 40 μM and the progression as concentration increase. It is thought that the survival of the mice is heavily dependent on the condition of the kidneys post-injection. It would appear that the mice in these experiments died of renal failure. The liver examination, however, revealed very little tissue damage that could be linked to death at any concentration. The lower dose mice have some small amount of kidney damage, typically in the form of shedding, but not enough to cause adverse effects over the long term.

Size-Dependent Clearance

Choi *et al.* has postulated that core size plays a critical role for the *in vivo* use of nanoparticles.[21] Based on this theory, mice were injected with particles separated using a 30 kDa MWCO filter. The small particles have a diameter of 3 ± 1 nm and the remaining particles are 4 ± 2 nm, showing they are statistically different sizes and more monodisperse. The smaller cores cause a much higher survival rate compared to the as synthesized TMPCs. At 0, 20, and 40 μM no mice fatalities occur. However, the 60 μM still require euthanizing after 3 days which mirrors the non-separated trials.

In following the format of the first study, organs were excised and analyzed for gold concentration. These organs exhibit a much more consistent trend in dose response,

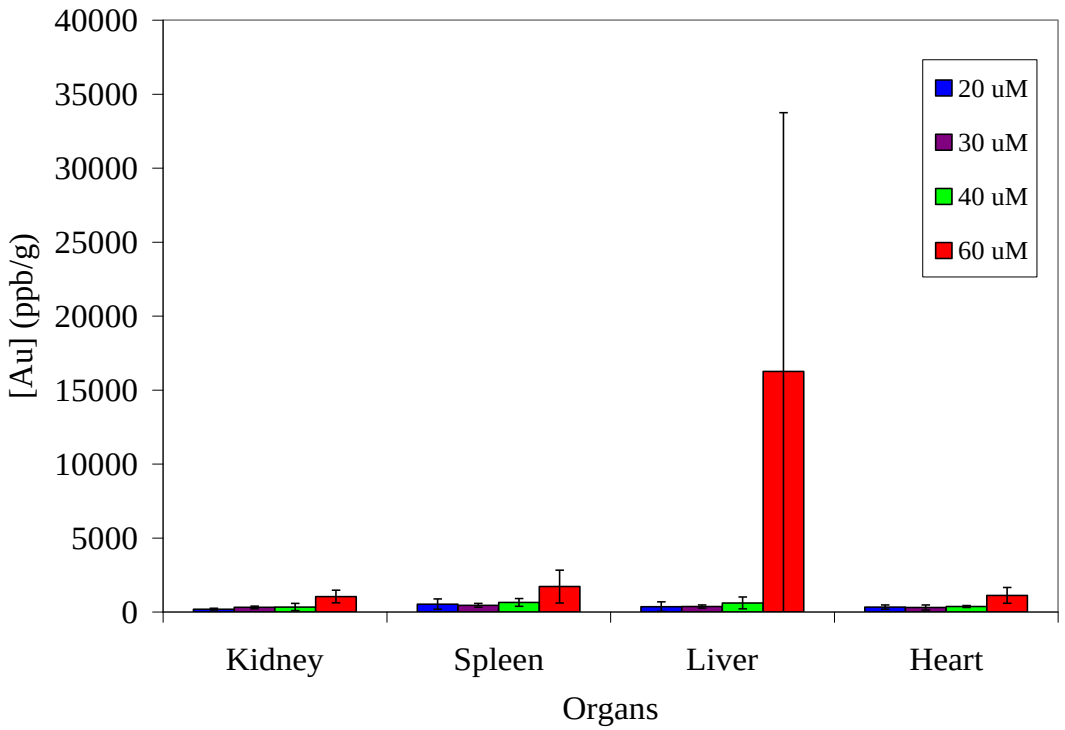

Figure 49. All the organs excised from the size separated dosing of the mice (n = 4 per group). Each group shows dosage dependent responses.

with the livers again showing the highest concentrations. The liver gold concentration shows a high overall quantity and also large deviation at the highest dosage ($1.6x10^4 \pm 1.7x10^4$ ppb), which could be attributed to when mice were euthanized. It can be thought that if the mice survive longer, the liver would have more time for uniform clearance of the TMPCs, but in the three day period the particles were heavily retained. Figure 49 shows the excised organs and their metal concentrations at each dosage. The heart, kidneys, and spleen all show fairly low levels with concentrations never exceeding 1500 ppb. The gold concentration in the blood and urine also change with the smaller size

particles. Within 24 hours of injection, the particles are totally cleared from the blood and urine, with a return to baseline levels (<20ppb). This is up to two days faster than the non-separated particles. Figure 43 shows the concentrations rapidly clearing in both the blood (50a) and urine (50b) during the sampling. In addition to faster clearance, the circulation concentration is lower in the blood over the 24 hour sampling period. Blood concentrations reach 68 ppb maximum, which is well under the quantities measured in the non-separated injections. Because blood levels are so low, it is expected that the bulk

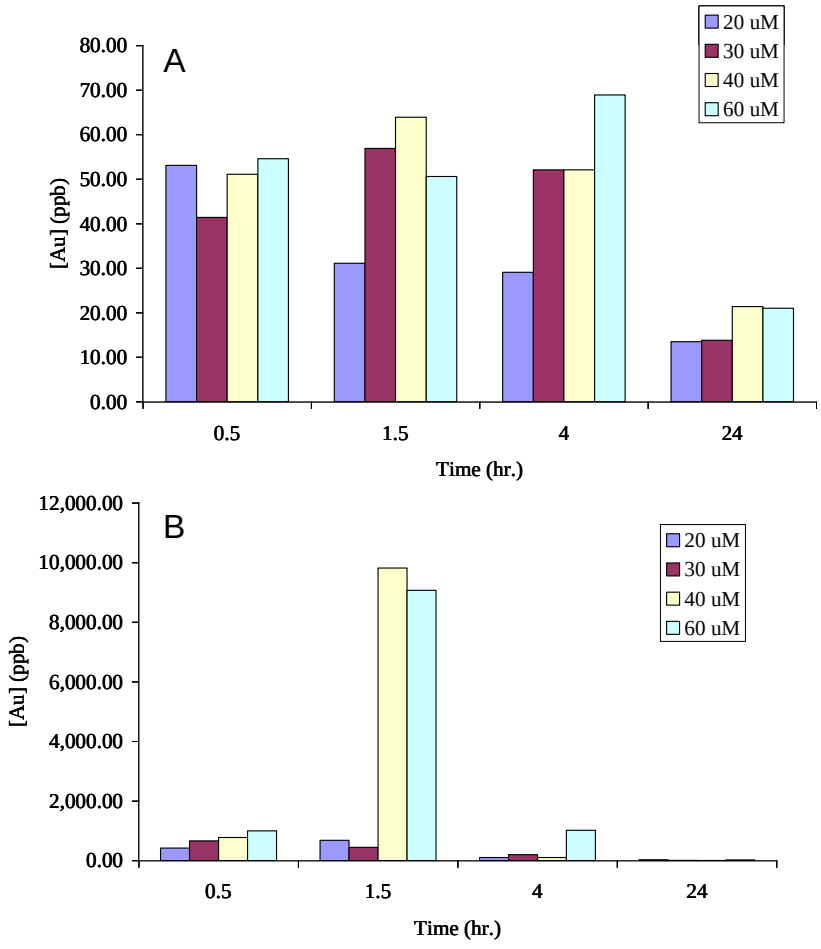

Figure 50. Concentration versus time profiles for the (a) blood and (b) urine clearance of smaller core TMPCs. The blood profile shows very low quantities of blood during the 24 hour period, while the urine levels spike at 1 ½ hours and rapidly return to pre-injection concentrations

of nanoparticles are cleared in the urine very quickly. The urine does show higher levels for the first four hours, compared to the non-separated TMPCs. Especially prominent are the spikes at 1 ½ hour. Possibly because the particles are smaller, the kidneys can tolerate these dosages with fewer negative consequences.

Conclusions

These experiments have shown that TMPCs can be tolerated *in vivo* at concentrations below 30 μM and lays the ground work for TMPCs as a viable platform for functionalized vaccine development *in vivo*. Using a mouse model, particles were quantified as they circulated and cleared the body. Typically, particles would clear the body after 96 hours, with levels returning to baseline concentrations. Organs were tested for gold retention after the mice were euthanized. The organ with the highest concentration was the liver, with the spleen and kidney closely matched. At higher doses, the spleen shows much more gold than any of the organs, most likely due to its blood to mass ratio.

Other biological markers show dosage dependent responses. There is an increased amount of RBCs, WBCs, and protein at the higher concentrations. This suggests that the kidneys were being damaged at those dosages. Also, the immunological changes were measured to see if the TMPCs illicit an immune response. No statistically relevant change was found over the course of four weeks in the RBC and WBC counts.

One more component to change was the size of the particles injected. A 3 nm particle was injected with a tighter dispersity than compared to the originally synthesized TMPCs. Smaller MPCs had better results, as the particles were cleared from the blood

and urine in less than 24 hours compared to the 96 hours for the non-separated injection. Also, the organs show a change in retention. The liver still shows the highest concentration, but all the organs in this set have higher amounts of gold than previously seen.

These particles could serve as a viable platform for future work in vaccines and imaging. So long as the dosage is kept low, the particles do not cause immunological changes or terminal damage. Through tailoring size, the dosage can be increased while minimizing any damages. It is interesting to note that these two prescribed starting materials, tiopronin (Thiola) and auric compounds do in fact show some toxicity as a combined nanomaterial. To decrease this toxicity further, a new formulation will be tested. The next step will be to functionalize the particles with different ligands to increase their efficacy for targeting and vaccination using PEGylated ligands that have been shown to increase circulation.[41] It is hoped this new particle will decrease toxicity while creating a scaffold for place-exchange reactions.

References

(1) Hostetler, M. J.; Templeton, A. C.; Murray, R. W. *Langmuir* **1999**, *15*, 3782-3789.

(2) Hostetler, M. J.; Wingate, J. E.; Zhong, C.-J.; Harris, J. E.; Vachet, R. W.; Clark, M. R.; Londono, J. D.; Green, S. J.; Stokes, J. J.; Wignall, G. D.; Glish, G. L.; Porter, M. D.; Evans, N. D.; Murray, R. W. *Langmuir* **1998**, *14*, 17-30.

(3) Templeton, A. C.; Chen, S.; Gross, S. M.; Murray, R. W. *Langmuir* **1999**, *15*, 66-76.

(4) Templeton, A. C.; Cliffel, D. E.; Murray, R. W. *J. Am. Chem. Soc.* **1999**, *121*, 7081-7089.

(5) Ranney, D. F. *Biochem. Pharmacol.* **2000**, *59*, 105-114.

(6) Cherukuri, P.; Gannon, C. J.; Leeuw, T. K.; Schmidt, H. K.; Smalley, R. E.; Curley, S. A.; Weisman, R. B. *Proc. Natl. Acad. Sci. U.S.A.* **2006**, *103*, 18882-18886.

(7) Hainfeld, J. F.; Slatkin, D. N.; Focella, T. M.; Smilowitz, H. M. *Br. J. Radiol.* **2006**, *79*, 248-253.
(8) Stroh, M.; Zimmer, J. P.; Duda, D. G.; Levchenko, T. S.; Cohen, K. S.; Brown, E. B.; Scadden, D. T.; Torchilin, V. P.; Bawendi, M. G.; Fukumura, D.; Jain, R. K. *Nature Medicine* **2005**, *11*, 678-682.
(9) Zimmer, J. P.; Kim, S.-W.; Ohnishi, S.; Tanaka, E.; Frangioni, J. V.; Bawendi, M. G. *J. Am. Chem. Soc.* **2006**, *128*, 2526-2527.
(10) Eck, W.; Craig, G.; Sigdel, A.; Ritter, G.; Old, L. J.; Tang, L.; Brennan, M. F.; Allen, P. J.; Mason, M. D. *ACS Nano* **2008**, *2*, 2263-2272.
(11) Everts, M.; Saini, V.; Leddon, J. L.; Kok, R. J.; Stoff-Khalili, M.; Preuss, M. A.; Millican, C. L.; Perkins, G.; Brown, J. M.; Bagaria, H.; Nikles, D. E.; Johnson, D. T.; Zharov, V. P.; Curiel, D. T. *Nano Lett.* **2006**, *6*, 587-591.
(12) Tkachenko, A. G.; Xie, H.; Coleman, D.; Glomm, W.; Ryan, J.; Anderson, M. F.; Franzen, S.; Feldheim, D. L. *J. Am. Chem. Soc.* **2003**, *125*, 4700-4701.
(13) Hainfeld, J. F.; Slatkin, D. N.; Smilowitz, H. M. *Phys. Med. Biol.* **2004**, *49*, 309-315.
(14) Khlebtsov, B.; Zharov, V.; Melnikov, A.; Tuchin, V.; Khlebtsov, N. *Nanotech* **2006**, *17*, 5167-5179.
(15) Taubert, A.; Napoli, A.; Meier, W. *Curr. Opin. Chem. Biol.* **2004**, *8*, 598-603.
(16) Devi, P. U.; Saharan, B. R. *Experientia* **1978**, *34*, 91-92.
(17) Ayene, I. S.; Al-Mehdi, A. B.; Fisher, A. B. *Arch. Biochem. Biophys.* **1993**, *303*, 307-312.
(18) Atamaca, G. *Yonsei Med J.* **2004**, *45*, 766-88.
(19) Shaw, C. F. *Chem. Rev.* **1999**, *99*, 2589-2600.
(20) Rae, C. S.; Khor, I. W.; Wang, Q.; Destito, G.; Gonzalez, M. J.; Singh, P.; Thomas, D. M.; Estrada, M. N.; Powell, E.; Finn, M. G.; Manchester, M. *Virology* **2005**, *343*, 224-235.
(21) Choi, H. S.; Liu, W.; Misra, P.; Tanaka, E.; Zimmer, J. P.; Ipe, B. I.; Bawendi, M. G.; Frangioni, J. V. *Nature Biotech* **2007**, *25*, 1165-1170.
(22) Owens, D. E.; Peppas, N. A. *Int. J. Pharm.* **2006**, *307*, 93-102.
(23) Chen, Z.; Meng, H.; Xing, G.; Chen, C.; Zhao, Y.; Jia, G.; Wang, T.; Yuan, H.; Ye, C.; Zhao, F.; Chai, Z.; Zhu, C.; Fang, X.; Ma, B.; Wan, L. *Toxicol. Lett.* **2006**, *163*, 109-120.
(24) Alexis, F.; Pridgen, E.; Molnar, L. K.; Farokhzad, O. C. *Mol. Pharmaceutics* **2008**, *5*, 505-515.
(25) Sonavane, G.; Tomoda, K.; Sano, A.; Ohshima, H.; Terada, H.; Makino, K. *Colloids Surf., B* **2008**, *65*, 1-10.
(26) Jong, W. H. D.; Hagens, W. I.; Krystek, P.; Burger, M. C.; Sips, A. J. A. M.; Geertsma, R. E. *Biomaterials* **2008**, *29*, 1912-1919.
(27) Inoue, K.-i.; Takano, H.; Yanagisawa, R.; Sakurai, M.; Ichinose, T.; Sadakane, K.; Yoshikawa, T. *Respir. Res.* **2005**, *6*.
(28) Wuelfing, W. P.; Gross, S. M.; Miles, D. T.; Murray, R. W. *J. Am. Chem. Soc.* **1998**, *120*, 12696-12697.
(29) Hillyer, J. F.; Albrecht, R. M. *J. Pharm. Sci.* **2001**, *90*, 1927-1936.

(30) Fitzpatrick, J. A. J.; Andreko, S. K.; Ernst, L. A.; Waggoner, A. S.; Ballou, B.; Bruchez, M. P. *Nano Lett.* **2009**, *9*, 2736-2741.
(31) Marquis, B. J.; Love, S. A.; Braun, K. L.; Haynes, C. L. *Analyst* **2009**, *134*, 425-439.
(32) Balaram, V. *Curr. Sci.* **1997**, *73*, 1019-1023.
(33) Gélinas, Y.; Youla, M.; Béliveau, R.; Schmit, J.-P. *Anal. Chim. Acta* **1992**, *269*, 115-122.
(34) Goullé, J.-P.; Mahieu, L.; Castermant, J.; Neveu, N.; Bonneau, L.; Lainé, G.; Bouige, D.; Lacroix, C. *Forensic Sci Int.* **2005**, *153*, 39-44.
(35) Scheffer, A.; Engelhard, C.; Sperling, M.; Buscher, W. *Anal. Bioanal. Chem* **2008**, *390*, 249-252.
(36) Brust, M.; Walker, M.; Bethell, D.; Schiffrin, D. J.; Whyman, R. *J. Chem. Soc., Chem Commun.* **1994**, 801-802.
(37) Templeton, A. C.; Wuelfing, W. P.; Murray, R. W. *Acc. Chem. Res.* **2000**, *33*, 27-36.
(38) Golde, W. T.; Gollobin, P.; Rodriguez, L. L. *LabAnimal* **2005**, *34*, 39-43.
(39) NIH 2005; Vol. 2008.
(40) Kurien, B. T.; Scofield, R. H. *Lab. Anim.* **1998**, *33*, 83-86.
(41) Niidome, T.; Yamagata, M.; Okamoto, Y.; Akiyama, Y.; Takahashi, H.; Kawano, T.; Katayama, Y.; Niidome, Y. *J. Controlled Release* **2006**, *114*, 343-347.